analytical chemistry

Article

pubs.acs.org/ac

Imidazolium-Based Ionic Liquid Surfaces for Biosensing

Mathieu Ratel,[†] Audrey Provencher-Girard,[†] Sandy Shuo Zhao,[†] Julien Breault-Turcot,[†] Jérémie Labrecque-Carbonneau,[†] Mathieu Branca,[†,‡] Joelle N. Pelletier,[†,§] Andreea R. Schmitzer,[†,*] and Jean-Francois Masson*[,†,▽]

[†]Département de Chimie, Université de Montréal, C.P. 6128 Succ. Centre-Ville, Montreal, Quebec, Canada H3C 3J7

[§]PROTEO, the Quebec Network for Protein Function, Structure and Engineering, Université Laval, Quebec, Canada G1V 0A6

[▽]Centre for Self-Assembled Chemical Structures (CSACS), McGill University, Montreal, Quebec, Canada H3A 2K6

Supporting Information

ABSTRACT: Ionic liquid self-assembled monolayers (SAM) were designed and applied for binding streptavidin, promoting affinity biosensing and enzyme activity on gold surfaces of sensors. The synthesis of 1-((+)-biotin)pentanamido)propyl)-3-(12-mercaptododecyl)-imidazolium bromide, a biotinylated ionic liquid (IL-biotin), which self-assembles on gold film, afforded streptavidin sensing with surface plasmon resonance (SPR). The IL-biotin-SAM efficiently formed a full streptavidin monolayer. The synthesis of 1-(carboxymethyl)-3-(mercapto-dodecyl)-imidazoliumbromide, a carboxylated IL (IL-COOH), was used to immobilize anti-IgG to create an affinity biosensor. The IL-COOH demonstrated efficient detection of IgG in the nanomolar concentration range, similar to the alkylthiols SAM and PEG. In addition, the IL-COOH demonstrated low fouling in crude serum, to a level equivalent to PEG. The IL-COOH was further modified with *N*,*N*′-bis (carboxymethyl)-L-lysine hydrate to bind copper ions and then, chelate histidine-tagged biomolecules. Human dihydrofolate reductase (hDHFR) was chelated to the modified IL-COOH. By monitoring enzyme activity in situ on the SPR sensor, it was revealed that the IL-COOH SAM improved the activity of hDHFR by 24% in comparison to classical SAM. Thereby, IL-SAM has been synthesized and successfully applied to three important biosensing schemes, demonstrating the advantages of this new class of monolayers.

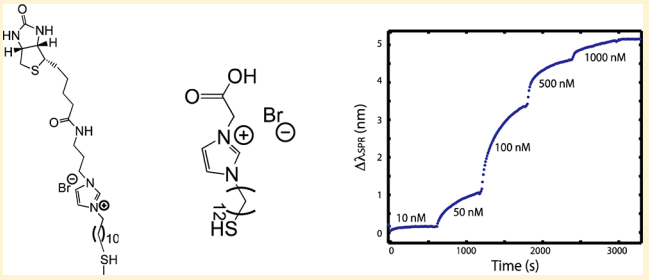

Self-assembled monolayers (SAMs) are increasingly used for biosensing to immobilize molecular recognition elements.[1] Indeed, the design of surfaces that bind an analyte target is particularly important for biosensors and affinity chromatography, while surfaces that resist nonspecific adsorption are particularly important for coating implants and artificial organs.[2] Optical and electrochemical biosensors are now widely popular for a plethora of applications in environmental, food safety, or biomedical applications.[3−7] Optical and electrochemical transducers often lack selectivity for specific analytes. The immobilization of highly active molecular receptors on the surface of the transducer, while minimizing nonspecific response from the sample matrix, is thus a common challenge to all biosensing technologies.

Ionic liquids (ILs) are generally defined as molten organic salts with a melting point below 100 °C. Enhanced biocatalytic transformations are a source of interest in bioanalytical sciences for ILs.[8] For example, fluorescence bioassays can be performed in ILs.[9] In addition, an extended potential window and enhanced electron transfer are characteristic of ILs.[10] For these reasons, the use of ILs in electrochemistry and for electrochemical biosensing has grown in popularity in the past decade.[11−13] Specifically, composite materials based on metal nanomaterials,[14] graphene,[15] graphite,[16,17] carbon nanotubes,[18−23] polymers,[24] chitosan,[25] and sol−gels[26] have demonstrated their utility in biosensors for hemoglobin, myoglobin, catalase, glucose oxidase, and horseradish peroxidase.[12] While the excellent properties of ILs in electrochemical sensing are widely demonstrated in the literature, there are few examples of optical sensors exploiting the properties of IL systems. The most prevalent example consists of using ILs in gas-sensing schemes.[27−31] Thus, the properties of ILs in optical sensing schemes remain poorly understood.

Optical sensing technologies constitute a major research field encompassing techniques that include surface plasmon resonance (SPR), plasmonic techniques, fluorescence, vibrational spectroscopies (Raman and infrared (IR)), and resonant waveguides, among others. Optical sensing technologies rely on fiber-optics, capillary waveguides, microsystems, refractive index sensing, and other spectroscopies.[32] These sensing technologies are based on active and functional surfaces. The modification of these surfaces with molecular receptors is essential to impart molecular selectivity to these techniques and requires modification of the sensor's surface with self-assembled monolayers (SAMs). While the overwhelming majority of surface chemistries are based on traditional organic compounds,

Received: February 6, 2013
Accepted: May 21, 2013

   dx.doi.org/10.1021/ac400386z | *Anal. Chem.* XXXX, XXX, XXX−XXX

there has been a recent interest in zwitterionic surfaces, because of their ultralow fouling in crude serum and other biofluids.[33−37] Thus, the zwitterionic nature of ILs, and their improved performance in biosensing, makes them ideal candidates for novel high-performance surface chemistries.

Task-specific ionic liquids (TS-ILs) are a class of ILs that bear a functional group designed to accomplish a chemical function.[38] IL-SAMs are a class of TS-ILs capable of binding to surfaces. In one application of TS-ILs, they require the introduction of a thiol on the alkyl chain of methylimidazolium to form a SAM on gold films.[39,40] ILs have also been used to stabilize gold nanoparticles.[41] While their properties remain little studied, the imidazolium cation exhibited anion exchange reactions, which was shown to control wettability of surfaces[40] and to form unexpected anion-exchange reactions with carbonate ILs.[42] IL-SAMs undergo temperature-dependent phase transitions when immobilized on gold films.[43] Hwang et al. have studied the electrochemical properties of IL-SAMs in a series of papers.[44−46] Despite these advances in understanding the properties of IL-SAMs, there are no reports of TS-ILs bearing functionalities suited for biosensing.

Biotin−streptavidin interactions have been studied extensively in the past decades.[47−57] The interaction of streptavidin and biotin have been well-characterized by a variety of methods, and that interaction is now commonly used in biosensing assays. Streptavidin binds to biotin with a very high dissociation constant ($K_d < 10^{-13}$ M). The multiple biotin binding sites of streptavidin make it well-suited to construct biosensors based on the strong affinity of these binding partners. Biosensors based on the streptavidin/biotin pair have been applied to the detection of antibiotics (e.g., chloramphenicol[53]), viruses (e.g., hepatitis C[57] and H1N1[58]), and cancer (e.g., prostate cancer[56]), among some examples. The synthesis of an IL-biotin would constitute an important model in biosciences.

It is generally known that chemical immobilization techniques often reduce the activity of molecular receptors. This decrease in activity of the receptor can be a serious limitation in biosensing, because it may lead to a reduction in sensitivity, as well as an increase of the limit of detection. These chemical immobilization techniques can block some active sites and sometime denature or alter the secondary structure of the immobilized protein. As detailed above, IL solutions are well-known to promote the activity of molecular receptors by maintaining the native conformation of the protein/enzyme. However, there is no study demonstrating the potential impact of an IL-SAM on the activity of an immobilized molecular receptor. In this paper, we present two important biosensing models based on the immobilization of active moelcular receptors on IL-SAMs. First, an affinity biosensor was based on an IL bearing a carboxylic acid functionality to immobilize anti-IgG selective to human IgG. Second, the IL modified with a NTA-like surface chemistry was used to immobilize human dihydrofolate reductase (hDHFR) to measure the influence of IL-SAM on the activity of an immobilized enzyme. These important examples of IL for biosensing demonstrate that the incorporation of IL is a promising approach for the development of improved surface chemistry.

EXPERIMENTAL DETAILS

Synthesis of an Ionic Liquid−Biotin (IL-Biotin). The synthesis of a biotinylated ionic liquid (1-((+)-biotin)-pentanamido)propyl)-3-(12-mercaptododecyl)-imidazolium bromide, compound ; see the Supporting Information for details) was carried out in six steps with an overall yield of 34% (see Scheme SI1 in the Supporting Information). Compound **8** was collected as a highly viscous translucent oil. Unless otherwise stated, all reactions were carried out under a nitrogen atmosphere.

Synthesis of an Ionic Liquid with a Carboxylic Acid. The synthesis of 1-(carboxymethyl)-3-(mercaptododecyl)-imidazoliumbromide, a carboxylated IL (IL-COOH, compound **11**) was carried out in four steps from imidazole (see Scheme SI2 in the Supporting Information for details). Compound **11** was obtained as a white solid with an overall yield of 29%. Unless otherwise stated, all reactions were carried out under a nitrogen atmosphere.

Contact Angle Measurements. The contact angles were measured for all samples using water as the solvent. A droplet of 30 μL of water was deposited on the IL-SAM. An image of the droplet was acquired with a digital camera, and the contact angles were measured from three independent samples using the computer software Image J.

Preparation of the SPR Sensors with IL-Biotin. The SPR sensors were manufactured on glass slides with dimensions of 22 mm × 22 mm. The glass slides were cleaned in hot piranha solution (70% H_2SO_4:30% H_2O_2) for 90 min and thoroughly cleaned with ultrapure water prior to the next step. [*Caution! Piranha solution is highly corrosive!*] Then, the glass slides were treated with a H_2O:NH_4OH:H_2O_2 solution (5:1:1) for 60 min in an ultrasonification bath and thoroughly cleaned with ultrapure water prior to the next step. The SPR sensor was created with the deposition of 1 nm of chromium and 50 nm of gold on the clean glass slide by sputter coating (Cressington, Model 308R).

The IL-biotin SAMs were formed by contacting the SPR sensor in a 2.5 mM ethanolic solution of 1-((+)-biotin)-pentanamido)propyl)-3-(12-mercaptododecyl)-imidazolium for a variable time between 3 s and 24 h. For monolayers using a diluent, a 2.5 mM ethanolic solution of either 1-dodecanethiol, cysteamine, 16-mercaptohexadecanoic acid, 11-mercaptoundecanoic acid, or 11-mercaptoundecanol was reacted for 24 h with the SPR sensor previously modified with IL-biotin. The SPR sensor was thereafter ready for SPR analysis of streptavidin. The IL-COOH SAM was formed overnight on a bare SPR sensor from a 5 mM ethanolic solution of compound **11**. The SPR sensors were washed in ethanol and dried with nitrogen. These SPR sensors were used as affinity sensors for IgG or for enzyme immobilization of His-tag hDHFR.

SPR Instrumentation. Surface plasmon resonance (SPR) experiments were performed on a custom-built instrument based on a dove prism and multiwavelength configuration.[59] The SPR sensors were put in optical contact with the prism using a RI-matching fluids, and a custom flow cell was fitted on the system to manage sample injection on the sensor. The sensorgrams were obtained from a 1 Hz acquisition rate of the *p*-polarized light, from which the dark spectrum was subtracted, and normalized with a previously stored reference spectrum consisting of the *s*-polarized light. Solutions were injected using a 1-mL syringe and measurement were done under static flow conditions. Data were collected with a portable spectrometer (Photon Control, Burnaby, BC, Canada) and processed with custom MatLab or Labview software, depending on the experiments. Graphical representation and extraction of the SPR data was also performed with these softwares.

Biosensor for Streptavidin. The interaction of biotin−streptavidin is commonly used in the construction of SPR

dx.doi.org/10.1021/ac400386z | *Anal. Chem.* XXXX, XXX, XXX−XXX

Scheme 1. On-Chip Synthesis of the *N,N′*-Bis-(carboxymethyl)-L-lysine IL-COOH SAM

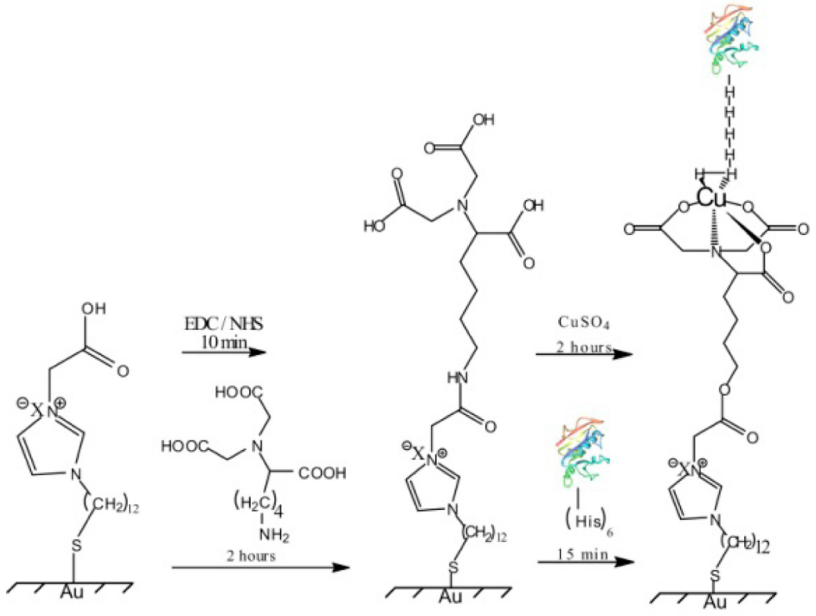

sensors. Thus, the interaction of native streptavidin from *Streptomyces avidinii* was assessed on the IL-biotin monolayer with high and low surface coverage of the IL-biotin. The SPR sensor functionalized with the IL-biotin SAM was placed on the SPR instrument. The sensor then was equilibrated with 1 mL of pH 7.4 PBS for 5 min. Streptavidin binding (>13 U/mg) was calibrated with solutions of increasing concentrations from 1 pM to 1 μM, in PBS. Each solution was injected (300 μL) and reacted for 10 min before the next concentration was injected. At the end of the calibration run, a final wash with 2 mL of PBS was performed to measure the final baseline. The SPR shift was measured as the difference between the SPR signal for the final 5 s of the injection of a given concentration, and the SPR signal of the initial baseline measurement in PBS. At least three measurements were performed on independent sensors to generate the average SPR response and standard deviation.

Affinity Biosensor for IgG. The model biological system was the antigoat immunoglobulin Gamma (anti-IgG) selective to human-IgG. This common model affords comparison with several other surface chemistries. Standard ethyl-(dimethylaminopropyl)carbodiimide (EDC) coupled to *N*-hydroxysuccinimide (NHS) chemistry was selected to immobilize anti-IgG to the C12-IL-COOH or C6-IL-COOH (compounds **11** and **12**). Every step was performed and recorded online on the SPR instrument. The sensor was hydrated for 2 min in ultrapure water by injecting 2 mL in the SPR flow cell. Then, 500 μL of a 1:1 solution of 350 mM EDC and 110 mM NHS activated the COOH group of IL-COOH for 4 min. The SPR sensor was washed with 1 mL of pH 4.5 PBS for 2 min. Then, 300 μL of a 1.5 μM anti-IgG (MW = 150 kDa) solution in pH 4.5 PBS was reacted with the SPR sensor for 15 min. The remaining NHS-activated sites were deactivated with 1 mL of 1 M ethanolamine (pH 8.5) for 5 min and washed with 1 mL of pH 7.4 PBS for 5 min. The calibration curve for human IgG was constructed by successive injections of 300 μL of human IgG (MW = 150 kDa) solutions at concentrations between 1 nM and 1 μM. Each concentration was reacted for 10 min and the SPR shift was measured as the difference between the SPR signal for the final 10 s of the injection of a given concentration, and the SPR signal of the initial baseline measurement in PBS. Finally, the SPR sensor was washed for 2 min with PBS. At least three measurements were performed on independent sensors to generate the average SPR response and standard deviation. The measurements were repeated on SPR sensors functionalized with 3-mercaptopropionic acid (3-MPA), 8-mercaptooctanoic acid (8-MOA), 11-mercaptoundecanoic acid (11-MUA), 16-mercaptohexadecanoic acid (16-MHA), and HS-C11-EG4-COOH (PEG).

Enzymatic Biosensor. Several biosensors are based on the immobilization of enzymes on surfaces. We recently demonstrated the value of hDHFR in a biosensor assay for methotrexate,[60] where the enzyme was in solution. We also previously adapted a method to monitor activity of histidine-tagged (His-tagged) hDHFR by spectrophotometry, directly on a SPR sensor placed in a 1-cm-path-length disposable plastic cuvette.[61,62] Here, activity of His-tagged hDHFR was monitored on the IL-SAM. Histidine-tagged hDHFR was obtained as previously described.[63] The SPR sensor was fabricated on a 9 mm × 9 mm glass slide. After the deposition of chromium and gold, the C12-IL-COOH monolayer was deposited as described above. The SAM then was activated with a 1:1 solution of 350 mM EDC and 110 mM NHS for 10 min. After the activation, the SPR sensors were rinsed and reacted with *N,N′*-bis (carboxymethyl)-L-lysine hydrate (7.5 mg/mL) for 2 h. Then, the monolayer was chelated with a copper sulfate pentahydrate solution (25 mg/mL) for 2 h (see Scheme SI3 in the Supporting Information). Finally, immediately before measuring the activity of hDHFR, a His-tagged hDHFR solution (50 μg/mL) was reacted on the SPR sensor for 15 min (Scheme 1).

The hDHFR activity was monitored according to the decrease in absorbance at 340 nm (Cary 100 Bio UV/vis spectrophotometer, Varian Canada) of a 1 mL mixture of 100 μM dihydrofolate (DHF) and 100 μM nicotinamide adenine dinucleotidephosphate (NADPH) in Tris buffer (pH 8). Substrates were quantified by spectrophotometry ($\varepsilon_{340\ nm}$ = 6200 M^{-1} cm^{-1} for NADPH and $\varepsilon_{282\ nm}$ = 28 400 M^{-1} cm^{-1} for

dx.doi.org/10.1021/ac400386z | *Anal. Chem.* XXXX, XXX, XXX−XXX

DHF). The SPR sensor modified with hDHFR then was introduced into the cuvette and the absorbance was monitored for 1 h. The decrease in absorbance indicated DHF (substrate) conversion in the presence of NADPH (cofactor), catalyzed by the hDHFR enzyme present on the IL-SAM surface.

RESULTS AND DISCUSSION

Synthesis of TS-IL for Biosensing. The synthesis of task-specific imidazolium salts was designed to obtain a nonconventional IL containing, in its structure, a ligand that can strongly and specifically bind a protein, when organized as a SAM on the gold surface (see Schemes SI1 and SI2 in the Supporting Information). The first family of TS-ILs prepared contains appended biotin groups, which allow the TS-IL to act as a recognition monolayer for streptavidin. Second, our attention turned to examining the use of carboxylic acid-functionalized ILs and their biomolecular stabilization properties.

Properties of IL-Biotin SAM. Steric interactions between neighboring molecular receptors can alter their capacity to bind the analyte. Receptors that are too close to each other may prohibit binding to the analyte. Thus, the surface chemistry must favor interaction between the analyte and the molecular receptor, such that binding can occur unimpeded. This is especially critical in the case of streptavidin−biotin interaction. Biotin, which is a small molecule, must be sufficiently spaced apart on the surface to permit interaction with streptavidin, a larger molecule (see Scheme SI3 in the Supporting Information). It was previously demonstrated that steric interactions prevented streptavidin from binding to a monolayer composed exclusively of biotin-modified SAM.[64,65] Biotinylated SAM must be used in a mixed SAM on the surface of the sensor to promote accessibility of the biotin groups and prevent nonspecific adsorption.[51] Binding kinetics of streptavidin also change depending on the fraction of the surface covered with a biotinylated SAM.[48] Thus, the properties of the IL-biotin must be investigated in binary SAMs.

While the relative solution concentration of each molecule loosely controls the surface concentration of binary self-assembled monolayers, the exact composition will differ from the concentration in solution.[66,67] The surface concentration depends on the rate of deposition, the chain length, and on the tail group of the molecule.[68] A pure solution of the IL-biotin was reacted for different times to control the fraction of IL-biotin present on a surface. The unreacted sites were capped with 1-dodecanethiol for 24 h to create a full monolayer, in order to expose the biotin group above the monolayer.[51] The surface coverage was estimated at different IL-biotin reaction times by applying a linear model between the SPR shift of the pure 1-dodecanethiol (t = 0 s) and pure IL-biotin (t = 24 h). As expected, the IL-biotin rapidly reacts with the surface to cover ∼40% of the surface (see Figure 1). Then, the reaction proceeds slowly as previously observed for other SAM on gold.[69] This two-step adsorption process corresponds to the rapid adsorption (within a few minutes) of other organic thiols, which precedes a slower step that lasts a few hours to attain a full monolayer.[70] While the surface coverage reaches 80%−90% within a few minutes for several organic thiols,[70] the IL-biotin reaches a more modest plateau at 40% surface coverage, which can be attributed to the bulkier IL-biotin tail group than that of a classical alkanethiol SAM.

As previously reported by Nelson et al.,[51] the tail group of the diluent monolayer also influences nonspecific adsorption of streptavidin on the surface of the sensor. Nonspecific

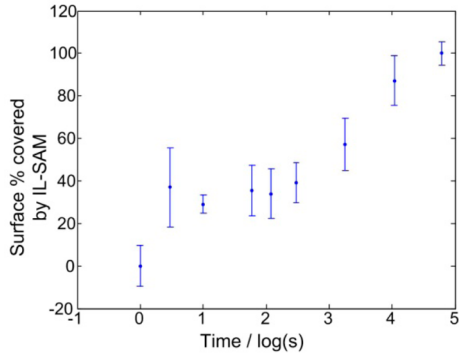

Figure 1. Surface coverage of the IL-biotin with 1-dodecanethiol, as measured by SPR.

interactions of analytes or interferents with a sensor can cause false positive responses or erroneous interpretation of data. Specifically, sensing technologies measuring bulk properties of analytes (such as mass or refractive index) are especially susceptible to interference from nonspecific adsorption. Hence, there has been a significant effort in understanding and preventing nonspecific interactions on sensors.[71] Nonspecific interactions of streptavidin can occur on surfaces, increasing the desorption rate of streptavidin[52] and on surfaces, providing poor resistance to nonspecific protein adsorption, such as methyl-terminated SAM.[47]

To evaluate nonspecific streptavidin adsorption on the SPR sensors, different alkanethiols with a shorter chain length than the IL-biotin were investigated to minimize nonspecific interactions of streptavidin to the SPR sensor. Methyl- (1-dodecanethiol), amino- (cysteamine), acid- (11-mercaptoundecanoic and 16-mercaptohexadecanoic acid), and alcohol-terminated (11-mercaptoundecanol) SAMs were exposed to 100 nM streptavidin to assess nonspecific interaction. As expected, 1-dodecanethiol led to significant nonspecific adsorption of streptavidin (181 ng/cm^2; see Table 1). The

Table 1. Nonspecific Adsorption of 100 nM Streptavidin on Different Alkanethiols

monolayer	$\Delta\lambda_{SPR}$ (nm)	Γ_{NSB} (ng/cm^2)
1-dodecanethiol	5.6 ± 0.4	181
cysteamine	0.6 ± 0.4	19
11-mercaptoundecanol	0.11 ± 0.05	3.5
11-MUA	0.18 ± 0.10	5.8
16-MHA	0.4 ± 0.3	13

nonspecific adsorption of streptavidin was on the same order of magnitude as specific adsorption of streptavidin using the IL-biotin, prohibiting the use of this molecule in a binary SAM for biosensing. SAM with polar tail groups significantly reduced nonspecific adsorption to 3.5−19 ng/cm^2, with the alcohol-terminated SAM performing best (see Table 1), which is in agreement with previous results on alkane SAM in other biofouling studies.[72] Hence, a binary monolayer of the IL-biotin and 11-mercaptoundecanol was selected for the streptavidin binding assays.

Calibration curves for streptavidin were constructed with two different reaction times for the IL-biotin, to compare the influence of the surface concentration of the biotin groups on streptavidin binding (see Figure 2). Reaction times of 5 min and 24 h were selected for the IL-biotin SAM formation to

dx.doi.org/10.1021/ac400386z | Anal. Chem. XXXX, XXX, XXX−XXX

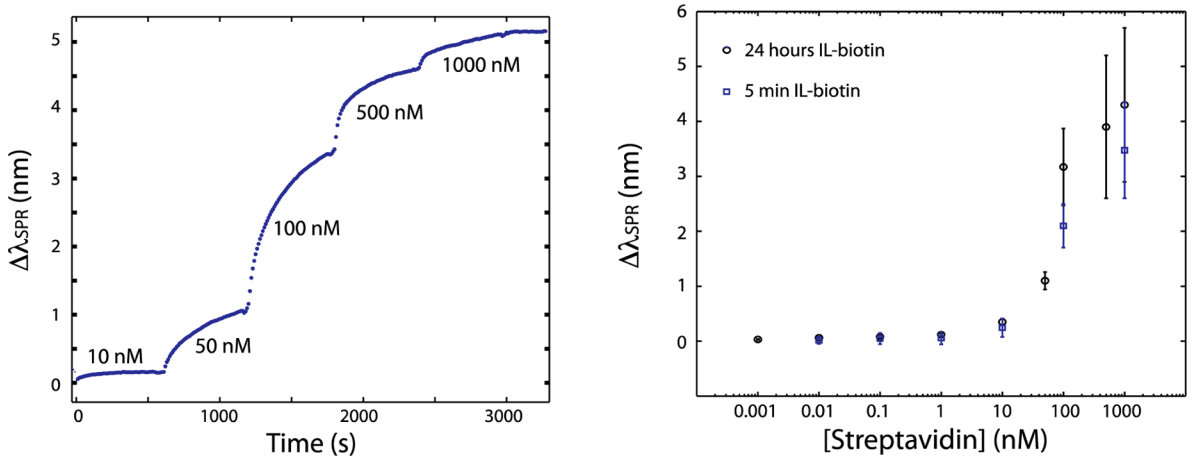

Figure 2. (Left) Adsorption isotherm for the streptavidin biosensor based on the IL-biotin. (Right) Calibration curves for the IL-biotin modified sensor. The sensor was reacted for 5 min (blue squares) and 24 h (black circles).

cover ~40% of the sensor with IL-biotin, or form a full monolayer of the IL-biotin, respectively. The consecutive injections of increasing concentrations of streptavidin clearly demonstrate the affinity of streptavidin for the IL-biotin (Figure 2, left). Modeling the response of the calibration curve with a Langmuir isotherm reveals that the dissociation constant (K_d) remained within error for both reaction times of the IL-biotin. Indeed, a surface prepared by reacting the IL-biotin for 5 min led to a K_d value of 89 nM, similar to the K_d value observed for the full IL-biotin monolayer (98 nM). The value of K_d is within the previously reported range of 10^{-11}–10^{-8} M for other biotinylated SAMs on SPR sensors.[49,52,73] The fluidic cell has a volume of ~50 μL, which equals to 3×10^{12} molecules in the fluidic cell at a streptavidin concentration of 100 nM, explaining that the K_d value observed is in the upper range of the reported values. The surface coverage of streptavidin was estimated from the maximum SPR shift for the calibration curve at a reaction time of 5 min. At saturation, streptavidin covers 1.1×10^{12} molecules/cm^2, corresponding to an average area of 93 nm^2 per molecule. Streptavidin has a unit cell of 9.84 nm × 9.84 nm × 12.58 nm,[55,56] which corresponds to a footprint of 97 nm^2, indicating that the IL-biotin leads to a full monolayer of streptavidin. Thus, the IL-biotin favors effective binding of streptavidin.

Affinity Biosensors with IL-COOH. The simplest and most common model for affinity biosensing involves the measurement of IgG with anti-IgG immobilized to the SPR sensor. The different SAMs were formed on the SPR sensor by reacting them overnight. The contact angle measurement of C6-IL-COOH (compound **12**; 36° ± 2°) and C12-IL-COOH (compound **11**; 40° ± 3°) revealed that the surfaces are relatively hydrophilic. In comparison, the contact angle of 1-(12-mercaptododecyl)-3-methyl-imidazolium carbonate (MDMI-HCO_3) was 42°–44°, very similar to those obtained here for the IL-COOHs. The different SAMs were identically activated with EDC-NHS to immobilize goat anti-IgG, followed by deactivation of the remaining NHS esters with ethanolamine. This standard procedure allows comparison between the IL-COOH monolayers and the alkylthiol and PEG surfaces.

Anti-IgG bound to the different surfaces to varying degrees of immobilization between 0.71 nm to 5.4 nm of SPR shift, corresponding to 20–153 ng/cm^2 (see Table 2). C6-IL-COOH and C12-IL-COOH bound anti-IgG at 76 and 105 ng/cm^2 respectively. The PEGylated surface led to the lowest surface concentration of anti-IgG of all surfaces tested, while no specific trend was observed for the alkylthiol and IL-COOH surfaces (see Table 2). The calibration curves for the alkylthiols and the IL-COOH nearly overlapped (see Figure 3), with a SPR response of nearly 3 nm at saturation. The PEGylated surface did not perform as well as these other surfaces with a maximum response of ~1 nm, but with a significantly lower surface concentration of anti-IgG. The K_d values extracted from these calibration curves were on the order of $(1.0–6.7) \times 10^{-7}$ M, with the lowest ones for the alkylthiol SAM and IL-COOH. The K_d values reported here are very similar to those observed for 3-MPA-HHHDD−OH (2.6×10^{-7} M[74]) and those for 11-MUA monolayers ($(0.54–6.2) \times 10^{-7}$ M).[75] PEG did not fare well, in comparison to the other SAM; it had the highest K_d value, although it was only marginally higher than most surfaces reported here. Detection limits were in the single-digit nanomolar range for all surface chemistries. The specificity of detection was confirmed by immobilizing rabbit antichicken IgY to the C12-Il-COOH monolayer. The calibration curve showed no response from concentrations of 1, 10, and 100 nM and a small, albeit measurable, response from 1000 nM IgG (see Figure 3). The response of the largest concentration is about an order of magnitude smaller than the specific response from the anti-IgG antibodies.

Table 2. Affinity Biosensors for IgG with Various Alkyl-, IL-, and PEG-SAMs

monolayer	$\Delta\lambda_{\text{Anti-IgG}}$ (nm)	$\Delta\lambda_{max}$ (nm)	K_D (nM)	activity (%)
3-MPA	5.4 ± 0.3	3.4 ± 0.1	100 ± 3	64 ± 4
8-MOA	3.6 ± 0.4	3.4 ± 0.2	200 ± 12	96 ± 10
11-MUA	3.2 ± 0.6	2.8 ± 0.2	200 ± 12	88 ± 14
16-MHA	4.1 ± 0.4	2.87 ± 0.09	200 ± 7	70 ± 7
IL-C6	2.7 ± 0.9	3.2 ± 0.1	200 ± 6	120 ± 23
IL-C12	3.7 ± 0.8	4.0 ± 0.2	582 ± 24	109 ± 16
PEG	0.71 ± 0.01	1.2 ± 0.1	667 ± 57	165 ± 6

The fraction of functional anti-IgG immobilized on the SPR sensor reveals whether the antibody is properly positioned on the SPR sensor to bind analytes. This parameter can be estimated from the SPR shift for anti-IgG and the maximum SPR shift obtained from the Langmuir modeling of the calibration curves. If all antibodies are functional when surface-bound, the SPR shift at saturation for IgG should be equal to the shift of the anti-IgG immobilization, because they have

dx.doi.org/10.1021/ac400386z | Anal. Chem. XXXX, XXX, XXX–XXX

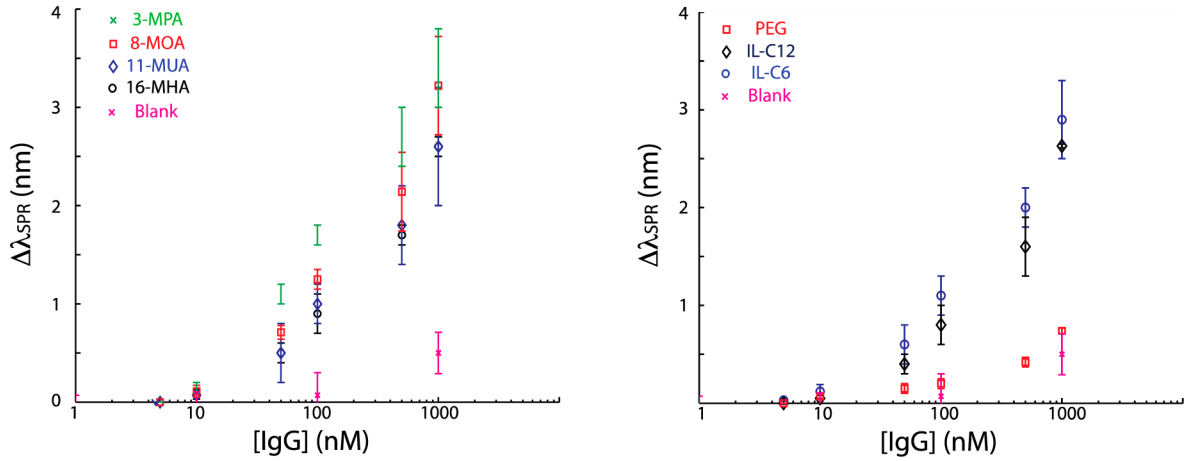

Figure 3. Calibration curves for the detection of IgG with various alkanethiol SAM (left) and IL-SAM or PEG (right).

Table 3. Activity of hDHFR Immobilized on Different Surface Chemistries

monolayer	density of hDHFR ($\times 10^{12}$ molecules/cm^2)	activity (pmol/min)	ratio (mol/mol hDHFR min^{-1})
IL-COOH	5.8	25 ± 9	2.1
3-MPA-LHDLHD−OH	3.9	11 ± 7	1.4
16-MHA	4.6	15.7 ± 3.3	1.7
PEG	7.7	5.3 ± 2.3	0.34

similar molecular weights. Otherwise, the number of molecules per square centimeter must be estimated for the antibody and the antigen to calculate the percentage of functional anti-IgG. The alkylthiol monolayers displayed the lowest binding activity, with results ranging from 64% to 96%, which is in agreement to our previously reported range for alkylthiol SAM.[76] IL-COOH and PEG fared better, at 109% and 120% of functionally bound antibodies for the IL-COOH and 165% for PEG (see Table 2). Results surpassing 100% signify that these monolayers promote divalent binding of IgG to the antibody, thus improving the apparent activity.

Nonspecific adsorption constitutes one of the major hurdles to overcome in SPR sensing.[71] As a nonspecific technique, SPR heavily relies on the selectivity of the surface chemistry and of the molecular receptor to quantitate analytes in crude biofluids. Because of the tendency of surfaces to bind a monolayer of protein when in the presence of crude biofluids,[72] the quantification of analytes in crude biofluids relies on the capacity to limit nonspecific adsorption of proteins contained in crude biofluids such as serum. Thus, crude serum containing ~70 mg/mL of proteins was injected on the C12-IL-COOH monolayer. The nonspecific interactions were measured at 99 ng/cm^2, a value similar to PEGylated surfaces under identical conditions.[77] For comparison, alkanethiol monolayers did significantly worse, with ~250−400 ng/cm^2 of protein adsorption in crude serum.[78] Nonspecific binding of crude serum was 45 ng/cm^2 with a biosensors functionalized with anti-IgG. Hence, detection of IgG spiked in bovine serum performed at 100 nM, which resulted in a shift of 1.1 ± 0.3 nm, which is significantly larger than the background signal of serum at 0.6 ± 0.1 nm, demonstrating the possibility of detecting proteins in crude serum with the C12-IL-COOH monolayer. The analytical performance of the IL-COOH clearly matches or surpasses that of PEG in a comparative study based on affinity biosensing.

Enzymatic Biosensors. Enzyme-based biosensors have revolutionized glucose monitoring.[79] They have been adapted to numerous detection schemes, mainly electrochemical[80] and optical.[81] ILs may promote enzyme activity, and biosensors have been developed with enzymes fixed on composite surfaces of conducting materials and ILs. Intuitively, one may wonder at the performance of a biosensor based on an enzyme immobilized on an IL-SAM.

Human dihydrofolate reductase (hDHFR) is the target of the widely administered chemotherapy drug, methotrexate (MTX). By binding strongly at the active site of hDHFR, MTX inhibits the conversion of dihydrofolate to tetrahydrofolate, which is essential for DNA synthesis and, thus, cellular proliferation. Our group has recently demonstrated that this enzyme functions in a biosensing scheme for quantification of MTX from clinical samples of patients undergoing chemotherapy.[60] Furthermore, the activity of the free hDHFR is maintained or slightly increased in solutions containing up to 10% 1-butyl-3-methylimidazolium with tetrafluoroborate as the counteranion (data not shown; manuscript in preparation). Finally, hDHFR can be immobilized in an active form by way of a His-tag, on gold surfaces modified with a nitrilotriacetic acid (NTA)-like monolayer.[61] Hence, hDHFR is a well-suited model for an enzymatic biosensor based on an IL-SAM.

The C12-IL-COOH and other monolayers (3-MPA-LHDLHD−OH, 16-MHA, and PEG) were activated with EDC-NHS to couple *N*,*N*′-bis (carboxymethyl)-L-lysine hydrate on the surface. These NTA-type monolayers bound Cu ions to chelate His-tagged hDHFR (see Scheme SI3 in the Supporting Information). The monolayers were formed on 9 mm × 9 mm, gold-coated coverslips, such that they could be inserted into spectrophotometry cuvettes. The SPR response during chelation of hDHFR to the surface provided a measure of the surface density on each SAM (see Table 3). hDHFR immobilization ranged from 3.9 × 10^{12} molecules/cm^2 to 7.7 × 10^{12} molecules/cm^2. The activity of the enzyme then was measured by monitoring the decrease in absorbance at 340 nm, similar to an assay for β-lactamase activity reported by Xu et al.[62] Here, the activity was quantified according to the decrease

dx.doi.org/10.1021/ac400386z | *Anal. Chem.* XXXX, XXX, XXX−XXX

in absorbance of the products (tetrahydrofolate and $NADP^+$), relative to the reactants (dihydrofolate and NADPH). The activity of the free hDHFR (not immobilized) was monitored as a positive control. A negative control consisting of the same reactants in the absence of the SPR sensor was subtracted from the data.

Activity of hDHFR was observed on each surface tested. The highest activity was observed for C12-IL-COOH at 25 ± 9 pmol/min, which is significantly greater than that for 16-MHA, 3-MPA-LHDLHD−OH, or PEG, which exhibited activities of 15.7 ± 3.3, 11 ± 7, and 5.3 ± 2.3 pmol/min, respectively (see Table 3). In comparison to the activity of 125 ng of free hDHFR in solution (630 ± 140 pmol/min), the surface-bound hDHFR was significantly less active. Lower activity is expected for an immobilized enzyme, because of slower hemispherical diffusion, and also, a possible loss of activity is observed, as a result of immobilization, or a lesser concentration of enzyme on the surface than in solution. Normalizing the activity with the surface concentration of hDHFR immobilized on the sensor assessed the relative performance of the different surfaces. The sensor with C12-IL-COOH resulted in a relative activity of 2.1 mol of dihydrofolate converted per mol of hDHFR, per minute (see Table 3). This relative activity for the IL-COOH is at least 24% greater than those observed on other surfaces. To date, enzyme activity had only been demonstrated with composite materials using electrochemical biosensors. To the best of our knowledge, the improved activity of hDHFR constitutes the first report of enhanced activity of an IL-SAM-immobilized enzyme. The IL-SAMs are clearly suited for biosensing with enhanced analytical properties.

CONCLUSIONS

Ionic liquid (IL) self-asembled monolayers based on long-chain alkyl imidazolium were synthesized with either biotin or carboxylic acid groups. 1-((((+)-biotin) pentanamido)propyl)-3-(12-mercaptododecyl)-imidazolium (IL-biotin) was synthesized with an overall yield of 34%. Mixed monolayers of the IL-biotin and 11-mercaptoundecanol reduced the nonspecific adsorption of streptavidin. Hence, a SPR sensor with dissociation constants of K_d = 89 and 98 nM for streptavidin resulted from the formation of the IL-biotin SAM. The relatively lower K_d was due to the low-volume fluidic cell of the SPR sensor, limiting the number of molecules available to bind the surface. Nonetheless, a full monolayer of streptavidin was formed on the SPR sensor, demonstrating the efficacy of the IL-biotin monolayer to construct a streptavidin-based biosensor. Typically, a diluent molecule must be used with biotinylated-SAM to effectively bind streptavidin, which was not necessary for the IL-biotin. 1-(Carboxymethyl)-3-(mercaptododecyl)-imidazolium bromide was synthesized with an overall yield of 29%. The IL-COOHs were suited for affinity biosensing, as demonstrated with IgG sensing. The K_d value observed was in good agreement with those reported in the literature and the analytical parameters were either similar or exceeded those of PEG. Nonspecific interaction of crude serum was equivalent to PEG, demonstrating the potential of the IL-COOH monolayer for biosensing in crude biofluids. Lastly, the IL-COOH was derived into a NTA-like surface, which was employed to immobilize hDHFR to create an enzyme biosensor. The sensor based on the IL-COOH showed higher enzyme activity than the other surface investigated, demonstrating the enhanced sensitivity of the IL-COOH-modified sensor. The results presented in this report clearly show the potential and advantages of using IL-SAM and lay the groundwork to create a novel class of monolayers for biosensing on gold surfaces.

ASSOCIATED CONTENT

Supporting Information

This material is available free of charge via the Internet at http://pubs.acs.org.

AUTHOR INFORMATION

Corresponding Author

*Tel.: +1 514 343 7342 (J.-F.M.), +1 514 343 6744 (A.R.S.). E-mail: jf.masson@umontreal.ca (J.-F.M.), schmitzer@umontreal.ca (A.R.S.).

Present Address

‡Present address: Laboratoire d'Électrochimie Moléculaire (LEM), Université Paris 7 Diderot—UMR 7591, 15 rue Jean-Antoine le Baïf, Bât. Lavoisier, 75013 Paris, France.

Notes

The authors declare no competing financial interest.

ACKNOWLEDGMENTS

The authors would like to thank NanoQuebec, the Canadian Space Agency, the Fonds Québécois de Recherche sur la Nature et les Technologies (FQRNT), the Canadian Foundation for Innovation, and the National Science and Engineering Research Council of Canada (NSERC) for providing funds to support this project.

REFERENCES

(1) Love, J. C.; Estroff, L. A.; Kriebel, J. K.; Nuzzo, R. G.; Whitesides, G. M. *Chem. Rev.* **2005**, *105* (4), 1103−1169.
(2) Mrksich, M.; Whitesides, G. M. *Annu. Rev. Biophys. Biomol. Struct.* **1996**, *25*, 55−78.
(3) Amine, A.; Mohammadi, H.; Bourais, I.; Palleschi, G. *Biosens. Bioelectron.* **2006**, *21* (8), 1405−1423.
(4) Baeumner, A. J. *Anal. Bioanal. Chem.* **2003**, *377* (3), 434−445.
(5) Rodriguez-Mozaz, S.; Lopez de Alda, M. J.; Barcelo, D. *Anal. Bioanal. Chem.* **2006**, *386* (4), 1025−1041.
(6) Shankaran, D. R.; Gobi, K. V. A.; Miura, N. *Sens. Actuators, B* **2007**, *121* (1), 158−177.
(7) Liu, Y.; Matharu, Z.; Howland, M. C.; Revzin, A.; Simonian, A. L. *Anal. Bioanal. Chem.* **2012**, *404* (4), 1181−1196.
(8) van Rantwijk, F.; Lau, R. M.; Sheldon, R. A. *Trends Biotechnol.* **2003**, *21* (3), 131−138.
(9) Baker, S. N.; Brauns, E. B.; McCleskey, T. M.; Burrell, A. K.; Baker, G. A. *Chem. Commun.* **2006**, *27*, 2851−2853.
(10) Liu, H.; Liu, Y.; Li, J. *Phys. Chem. Chem. Phys.* **2010**, *12* (8), 1685−1697.
(11) Opallo, M.; Lesniewski, A. *J. Electroanal. Chem.* **2011**, *656* (1−2), 2−16.
(12) Shiddiky, M. J. A.; Torriero, A. A. J. *Biosens. Bioelectron.* **2011**, *26* (5), 1775−1787.
(13) Wei, D.; Ivaska, A. *Anal. Chim. Acta* **2008**, *607* (2), 126−135.
(14) Franzoi, A. C.; Vieira, I. C.; Dupont, J.; Scheeren, C. W.; de Oliveira, L. F. *Analyst* **2009**, *134* (11), 2320−2328.
(15) Zhang, Q.; Wu, S.; Zhang, L.; Lu, J.; Verproot, F.; Liu, Y.; Xing, Z.; Li, J.; Song, X.-M. *Biosens. Bioelectron.* **2011**, *26* (5), 2632−2637.
(16) Franzoi, A. C.; Dupont, J.; Spinelli, A.; Vieira, I. C. *Talanta* **2009**, *77* (4), 1322−1327.
(17) Franzoi, A. C.; Migowski, P.; Dupont, J.; Vieira, I. C. *Anal. Chim. Acta* **2009**, *639* (1−2), 90−95.
(18) Kachoosangi, R. T.; Musameh, M. M.; Abu-Yousef, I.; Yousef, J. M.; Kanan, S. M.; Xiao, L.; Davies, S. G.; Russell, A.; Compton, R. G. *Anal. Chem.* **2009**, *81* (1), 435−442.

(19) Wang, Q.; Tang, H.; Me, Q.; Tan, L.; Zhang, Y.; Li, B.; Yao, S. *Electrochim. Acta* **2007**, *52* (24), 6630−6637.
(20) Yang, Y.-C.; Dong, S.-W.; Shen, T.; Jian, C.-X.; Chang, H.-J.; Li, Y.; Zhou, J.-X. *Electrochim. Acta* **2011**, *56* (17), 6021−6025.
(21) Zhu, Z.; Qu, L.; Li, X.; Zeng, Y.; Sun, W.; Huang, X. *Electrochim. Acta* **2010**, *55* (20), 5959−5965.
(22) Gopalan, A. I.; Lee, K.-P.; Ragupathy, D. *Biosens. Bioelectron.* **2009**, *24* (7), 2211−2217.
(23) Zhao, Y.; Liu, H.; Kou, Y.; Li, M.; Zhu, Z.; Zhuang, Q. *Electrochem. Commun.* **2007**, *9* (10), 2457−2462.
(24) Zhang, J.; Lei, J.; Liu, Y.; Zhao, J.; Ju, H. *Biosens. Bioelectron.* **2009**, *24* (7), 1858−63.
(25) Xi, F.; Liu, L.; Wu, Q.; Lin, X. *Biosens. Bioelectron.* **2008**, *24* (1), 29−34.
(26) Pauliukaite, R.; Doherty, A. P.; Murnaghan, K. D.; Brett, C. M. A. *Electroanalysis* **2008**, *20* (5), 485−490.
(27) Aydogdu, S.; Ertekin, K.; Suslu, A.; Ozdemir, M.; Celik, E.; Cocen, U. *J. Fluoresc.* **2011**, *21* (2), 607−613.
(28) Borisov, S. M.; Waldhier, M. C.; Klimant, I.; Wolfbeis, O. S. *Chem. Mater.* **2007**, *19* (25), 6187−6194.
(29) Celik, S.; Ertekin, K.; Gundogdu, C.; Ergun, Y.; Alp, S. *Spectrosc. Lett.* **2012**, *45* (1), 74−83.
(30) Oter, O.; Ertekin, K.; Topkaya, D.; Alp, S. *Anal. Bioanal. Chem.* **2006**, *386* (5), 1225−1234.
(31) Oter, O.; Ertekin, K.; Topkaya, D.; Alp, S. *Sens. Actuators, B* **2006**, *117* (1), 295−301.
(32) Wolfbeis, O. S. *Anal. Chem.* **2008**, *80* (12), 4269−4283.
(33) Vaisocherova, H.; Zhang, Z.; Yang, W.; Cao, Z. Q.; Cheng, G.; Taylor, A. D.; Piliarik, M.; Homola, J.; Jiang, S. Y. *Biosens. Bioelectron.* **2009**, *24* (7), 1924−1930.
(34) Vaisocherova, H.; Yang, W.; Zhang, Z.; Cao, Z. Q.; Cheng, G.; Piliarik, M.; Homola, J.; Jiang, S. Y. *Anal. Chem.* **2008**, *80* (20), 7894−7901.
(35) Sun, Q.; Su, Y. L.; Ma, X. L.; Wang, Y. Q.; Jiang, Z. Y. *J. Membr. Sci.* **2006**, *285* (1−2), 299−305.
(36) Chen, S. F.; Cao, Z. Q.; Jiang, S. Y. *Biomaterials* **2009**, *30* (29), 5892−5896.
(37) Chang, Y.; Chen, S. F.; Zhang, Z.; Jiang, S. Y. *Langmuir* **2006**, *22* (5), 2222−2226.
(38) Lee, S. G. *Chem. Commun.* **2006**, *10*, 1049−1063.
(39) Lee, B. S.; Lee, S. *Bull. Korean Chem. Soc.* **2004**, *25* (10), 1531−1537.
(40) Lee, B. S.; Chi, Y. S.; Lee, J. K.; Choi, I. S.; Song, C. E.; Namgoong, S. K.; Lee, S. G. *J. Am. Chem. Soc.* **2004**, *126* (2), 480−481.
(41) Garcia-Etxarri, A.; Aizpurua, J.; Molina-Aldareguia, J.; Marcilla, R.; Adolfo Pomposo, J.; Mecerreyes, D. *Frontiers Phys. China* **2010**, *5* (3), 330−336.
(42) Ratel, M.; Branca, M.; Breault-Turcot, J.; Zhao, S. S.; Chaurand, P.; Schmitzer, A. R.; Masson, J.-F. *Chem. Commun.* **2011**, *47* (38), 10644−10646.
(43) Branca, M.; Correia-Ledo, D.; Bolduc, O. R.; Ratel, M.; Schmitzer, A. R.; Masson, J.-F. *Phys. Chem. Chem. Phys.* **2011**, *13* (25), 12015−12023.
(44) Chi, Y. S.; Hwang, S.; Lee, B. S.; Kwak, J.; Choi, I. S.; Lee, S. *Langmuir* **2005**, *21* (10), 4268−4271.
(45) Hwang, S.; Chi, Y. S.; Lee, B. S.; Lee, S. G.; Choi, I. S.; Kwak, J. *Chem. Commun.* **2006**, *42* (2), 183−185.
(46) Hwang, S.; Lee, B. S.; Chi, Y. S.; Kwak, J.; Choi, I. S.; Lee, S. G. *Electrochim. Acta* **2008**, *53* (5), 2630−2636.
(47) Jung, L. S.; Nelson, K. E.; Campbell, C. T.; Stayton, P. S.; Yee, S. S.; Perez-Luna, V.; Lopez, G. P. *Sens. Actuators, B* **1999**, *54* (1−2), 137−144.
(48) Jung, L. S.; Nelson, K. E.; Stayton, P. S.; Campbell, C. T. *Langmuir* **2000**, *16* (24), 9421−9432.
(49) Liang, H. M.; Miranto, H.; Granqvist, N.; Sadowski, J. W.; Viitala, T.; Wang, B. C.; Yliperttula, M. *Sens. Actuators, B* **2010**, *149* (1), 212−220.
(50) Lind, K.; Kubista, M. *J. Immunol. Methods* **2005**, *304* (1−2), 107−116.
(51) Nelson, K. E.; Gamble, L.; Jung, L. S.; Boeckl, M. S.; Naeemi, E.; Golledge, S. L.; Sasaki, T.; Castner, D. G.; Campbell, C. T.; Stayton, P. S. *Langmuir* **2001**, *17* (9), 2807−2816.
(52) Perez-Luna, V. H.; O'Brien, M. J.; Opperman, K. A.; Hampton, P. D.; Lopez, G. P.; Klumb, L. A.; Stayton, P. S. *J. Am. Chem. Soc.* **1999**, *121* (27), 6469−6478.
(53) Sai, N.; Chen, Y. P.; Liu, N.; Yu, G. G.; Su, P.; Feng, Y.; Zhou, Z. J.; Liu, X. Y.; Zhou, H. Y.; Gao, Z. X.; Ning, B. A. *Talanta* **2010**, *82* (4), 1113−1121.
(54) Spinke, J.; Liley, M.; Schmitt, F. J.; Guder, H. J.; Angermaier, L.; Knoll, W. *J. Chem. Phys.* **1993**, *99* (9), 7012−7019.
(55) Weber, P. C.; Cox, M. J.; Salemme, F. R.; Ohlendorf, D. H. *J. Biol. Chem.* **1987**, *262* (26), 12728−12729.
(56) Weber, P. C.; Ohlendorf, D. H.; Wendoloski, J. J.; Salemme, F. R. *Science* **1989**, *243* (4887), 85−88.
(57) Xie, L.; Guang, Y. P.; Liu, F.; Shi, H. B.; Yan, L.; Lou, J. L. *Afr. J. Microbiol. Res.* **2011**, *5* (1), 28−33.
(58) Shao, H. X.; Ye, J. Q.; Vincent, A. L.; Song, H. C.; Hickman, D.; Qin, A. J.; Lamichhane, C.; Perez, D. R. *Influenza Other Respir. Viruses* **2011**, *5*, 138−142.
(59) Bolduc, O. R.; Live, L. S.; Masson, J. F. *Talanta* **2009**, *77* (5), 1680−1687.
(60) Zhao, S. S.; Bichelberger, M. A.; Colin, D. Y.; Robitaille, R.; Pelletier, J. N.; Masson, J.-F. *Analyst* **2012**, *137* (20), 4742−4750.
(61) Bolduc, O. R.; Lambert-Lanteigne, P.; Colin, D. Y.; Zhao, S. S.; Proulx, C.; Boeglin, D.; Lubell, W. D.; Pelletier, J. N.; Fethiere, J.; Ong, H.; Masson, J.-F. *Analyst* **2011**, *136* (15), 3142−3148.
(62) Xu, F.; Zhen, G.; Yu, F.; Kuennemann, E.; Textor, M.; Knoll, W. *J. Am. Chem. Soc.* **2005**, *127* (38), 13084−13085.
(63) Volpato, J. P.; Fossati, E.; Pelletier, J. N. *J. Mol. Biol.* **2007**, *373*, 599−611.
(64) Haussling, L.; Knoll, W.; Ringsdorf, H.; Schmitt, F. J.; Yang, J. L. *Makromol. Chem., Macromol. Symp.* **1991**, *46*, 145−155.
(65) Haussling, L.; Ringsdorf, H.; Schmitt, F. J.; Knoll, W. *Langmuir* **1991**, *7* (9), 1837−1840.
(66) Bain, C. D.; Whitesides, G. M. *Science* **1988**, *240* (4848), 62−63.
(67) Bain, C. D.; Whitesides, G. M. *J. Am. Chem. Soc.* **1988**, *110* (11), 3665−3666.
(68) Laibinis, P. E.; Fox, M. A.; Folkers, J. P.; Whitesides, G. M. *Langmuir* **1991**, *7* (12), 3167−3173.
(69) Schwartz, D. K. *Annu. Rev. Phys. Chem.* **2001**, *52* (1), 107−137.
(70) Bain, C. D.; Troughton, E. B.; Tao, Y. T.; Evall, J.; Whitesides, G. M.; Nuzzo, R. G. *J. Am. Chem. Soc.* **1989**, *111* (1), 321−335.
(71) Blaszykowski, C.; Sheikh, S.; Thompson, M. *Chem. Soc. Rev.* **2012**, *41* (17), 5599−5612.
(72) Ostuni, E.; Chapman, R. G.; Holmlin, R. E.; Takayama, S.; Whitesides, G. M. *Langmuir* **2001**, *17* (18), 5605−5620.
(73) Haes, A. J.; Van Duyne, R. P. *J. Am. Chem. Soc.* **2002**, *124* (35), 10596−10604.
(74) Bolduc, O. R.; Pelletier, J. N.; Masson, J.-F. *Anal. Chem.* **2010**, *82* (9), 3699−3706.
(75) Dong, Y.; Wilkop, T.; Xu, D.; Wang, Z.; Cheng, Q. *Anal. Bioanal. Chem.* **2008**, *390* (6), 1575−1583.
(76) Battaglia, T. M.; Masson, J. F.; Sierks, M. R.; Beaudoin, S. P.; Rogers, J.; Foster, K. N.; Holloway, G. A.; Booksh, K. S. *Anal. Chem.* **2005**, *77* (21), 7016−7023.
(77) Bolduc, O. R.; Clouthier, C. M.; Pelletier, J. N.; Masson, J.-F. *Anal. Chem.* **2009**, *81* (16), 6779−6788.
(78) Masson, J. F.; Battaglia, T. M.; Cramer, J.; Beaudoin, S.; Sierks, M.; Booksh, K. S. *Anal. Bioanal. Chem.* **2006**, *386* (7−8), 1951−1959.
(79) Wang, J. *Chem. Rev.* **2008**, *108* (2), 814−825.
(80) Pumera, M.; Sanchez, S.; Ichinose, I.; Tang, J. *Sens. Actuators, B* **2007**, *123* (2), 1195−1205.
(81) Monk, D. J.; Walt, D. R. *Anal. Bioanal. Chem.* **2004**, *379* (7−8), 931−945.